Molecular Microbiology (2004) **52**(4), 1029–1044 doi:10.1111/j.1365-2958.2004.04040.x

Proteomic screening and identification of differentially distributed membrane proteins in *Escherichia coli*

Erh-Min Lai,[†‡] Usha Nair,[‡] Nikhil D. Phadke and Janine R. Maddock*

Department of Molecular, Cellular and Developmental Biology, University of Michigan, 830 North University, Ann Arbor, MI 48109, USA.

Summary

Bacteria show asymmetric subcellular distribution of many proteins involved in diverse cellular processes such as chemotaxis, motility, actin polymerization, chromosome partitioning and cell division. In many cases, the specific subcellular localization of these proteins is critical for proper regulation and function. Although cellular organization of the bacterial cell clearly plays an important role in cell physiology, systematic studies to uncover asymmetrically distributed proteins have not been reported previously. In this study, we undertook a proteomics approach to uncover polar membrane proteins in *Escherichia coli*. We identified membrane proteins enriched in *E. coli* minicells using a combination of two-dimensional electrophoresis and mass spectrometry. Among a total of 173 membrane protein spots that were consistently detected, 36 spots were enriched in minicell membranes, whereas 15 spots were more abundant in rod cell membranes. The minicell-enriched proteins included the inner membrane proteins MCPs, AtpA, AtpB, YiaF and AcrA, the membrane-associated FtsZ protein and the outer membrane proteins YbhC, OmpW, Tsx, Pal, FadL, OmpT and BtuB. We immunolocalized two of the minicell-enriched proteins, OmpW and YiaF, and showed that OmpW is a *bona fide* polar protein whereas YiaF displays a patchy membrane distribution with a polar and septal bias.

Introduction

Bacterial cells display a remarkably sophisticated level of organization with many proteins being asymmetrically localized to specific cellular locations. In some cases, protein localization appears to be relatively static. Often, the asymmetry of these proteins and protein complexes can be attributed to the location of assembled external structures such as pili, flagella and stalks. In other cases, the function of polar protein localization is a mystery. A well-studied example of this class of asymmetric proteins are the *Escherichia coli* membrane chemoreceptors (MCPs) and associated cytoplasmic proteins. In *E. coli*, components of the chemotaxis machinery are localized predominantly to either one or both poles of the cell (Maddock and Shapiro, 1993; Sourjik and Berg, 2000; Shiomi *et al*., 2002; Cantwell *et al*., 2003). Furthermore, the MCPs aggregate in clusters at the poles (Maddock and Shapiro, 1993). This aggregation is largely reduced in the absence of CheA and CheW, suggesting a requirement for the MCP–CheA–CheW ternary complex for their optimal clustering (Maddock and Shapiro, 1993). The chemoreceptors are also predominantly clustered at the poles in a wide range of bacteria and archaea (Alley *et al*., 1992; Maddock and Shapiro, 1993; Harrison *et al*., 1999; Gestwicki *et al*., 2000; Kirby *et al*., 2000), indicating that polar clustering is evolutionarily conserved and likely to be important for chemotaxis function.

Some bacterial proteins are dynamically localized to specific cellular addresses in a cell cycle-dependent manner. A number of these proteins are required for the process of cell division such as the tubulin-like protein FtsZ (Bi and Lutkenhaus, 1991) and its spatial regulators, MinC, MinD (Bi and Lutkenhaus, 1993; Hu and Lutkenhaus, 1999) and MinE (Raskin and de Boer, 1997). Others are important for chromosome partitioning (for a review, see Draper and Gober, 2002). Particularly intriguing are the two-component regulatory proteins in *Caulobacter crescentus* that undergo dynamic cell cycle-dependent polar localization (reviewed by Shapiro *et al*., 2002). In this case, the temporal and spatial localization of specific histidine kinases and response regulators is critical for their function.

Yet another group of asymmetric proteins localize specifically in response to an external cue. The type III secretion system of *Yersinia pestis* injects a diverse array of effector proteins directly into the eukaryotic cytosol (for a review, see Cornelis, 2002). The type III secretion apparatus is made of ≈25 proteins that resemble a basal body of a flagellum with a small needle protruding

Accepted 16 January, 2004. *For correspondence. E-mail maddock@umich.edu; Tel. (+1) 734 936 8068; Fax (+1) 734 647 0884. [†]Present address: Institute of Botany, Academia Sinica, Nankang, Taipei, Taiwan 115. [‡]These authors contributed equally to this work.

from the bacterial surface (Kubori *et al*., 1998). Contact between the pathogen and the eukaryotic cell induces the transfer of YopE within the contact regions of bacterial and eukaryotic cells (Rosqvist *et al*., 1994). Similarly, bacterial conjugation requires physical contact between the donor and recipient bacteria. The contact regions and subsequent transfer of DNA occur at any position for both bacteria with the exception of pole-to-pole transfer (Lawley *et al*., 2002). Thus, the active conjugative apparatus is formed at virtually any position on the donor and recipient cell. In both examples, it is not known whether these complexes are synthesized *de novo* at the site of cell–cell contact or whether only specific inactive complexes are activated upon cell contact. Regardless, the cellular location of these complexes is critical for their function.

For most polar proteins, the mechanism by which they are targeted to the cell poles is not known. In one instance, IcsA, an actin polymerization protein in *Shigella flexneri*, is inserted directly into the polar membrane (Steinhauer *et al*., 1999). An IcsA-specific protease, IcsP, specifically degrades IcsA that spreads to the lateral membrane, thereby increasing its concentration at the poles (Steinhauer *et al*., 1999). In another example, SpoIVFB, a sporulation membrane protein in *Bacillus subtilis*, originally localizes to the cytoplasmic membrane of the mother cell. During sporulation, it reaches the polar septum by diffusion, migrates with the septal membrane during engulfment and is captured in the outer forespore membrane (Rudner *et al*., 2002). Regardless of the mechanism of initially establishing polarity, there must also be a mechanism to retain polar proteins at their appropriate cellular location. The nature of these 'polar anchors' is currently unknown. Likely candidates include other polar proteins, the composition of the membrane or peptidoglycan at the cell poles.

The list of asymmetrically localized proteins is increasing, in large part because of the use of green fluorescent protein (GFP) fusions. However, these studies tend to focus on proteins suspected to have non-random localization patterns such as those involved in cell division or polar organelle development. Thus, it is not clear whether polar and/or dynamically localized proteins represent a minor class of specialized proteins or whether a larger number of membrane proteins are polar. In this study, we took advantage of *E. coli* minicell mutants, in combination with proteomic tools, to identify potential polar membrane proteins. In wild-type *E. coli*, the self-assembly of FtsZ at the mid-cell position, along with the recruitment of other cell division proteins, ultimately results in two equal-sized, rod daughter cells (reviewed by Errington *et al*., 2003). In the absence of the Min system (encoded by the *minC*, *minD* and *minE* genes), the division septa occur not only in the middle but also at the poles of the cell, resulting in viable, elongated rod cells and small, spherical, anucleate minicells (Adler *et al*., 1967; Bi and Lutkenhaus, 1993). As minicells are essentially composed of two poles without lateral membrane, we predicted that they would be enriched in polar proteins, whereas the daughter rod cells would be enriched in lateral membrane proteins. One limitation to using the minicell system to identify polar proteins is that it is difficult to distinguish proteins that are truly polar from those that transiently associate with septation proteins during cell division. Additionally, some proteins may be enriched in minicells because either their own stability or that of their mRNAs may be enhanced in this environment.

In this study, we performed a comprehensive analysis of the membrane proteome of minicells and rod cells from *E. coli* with the goal of expanding the list of asymmetrically localized proteins. Using a combination of high-resolution two-dimensional gel electrophoresis and mass spectrometry, we identified 36 protein spots that were enriched in minicell membranes and 15 proteins spots enriched in rod cell membranes. We consider these to be protein candidates for asymmetrically localized proteins. Indeed, the localization patterns of two proteins enriched in minicell membranes, OmpW and YiaF, were shown to be polar and polar patchy respectively.

Results

Comparison of membrane protein profiles between minicells and rod cells by one-dimensional electrophoresis SDS–PAGE

Many early studies comparing the protein composition of minicells and rod cells reported no differences (Wilson and Fox, 1971; Green and Schaechter, 1972; Goodell and Schwarz, 1977), whereas assays based on enzymatic activity did show differences (Dvorak *et al*., 1970). One possibility is that the vast majority of proteins are evenly distributed, and visualization of the minor asymmetric proteins was obscured in these assays. Here, we examined the protein profiles of purified membrane preparations of daughter minicells and rod cells from the same cell cultures. We also focused on a reduced protein mixture by examining only membrane proteins and using a sodium carbonate wash (Molloy *et al*., 2000) to remove the majority of peripheral membrane proteins.

Minicells and rod cells were purified from an *E. coli* minicell mutant (X-1488) grown at either 30°C or 37°C by differential centrifugation. The purity of the resulting cell types was assayed by light microscopy. Whereas the starting culture was a mixture of rod cells and minicells (Fig. 1A), after differential centrifugation, we obtained relatively pure populations of rod cells (Fig. 1B) and minicells (Fig. 1C).

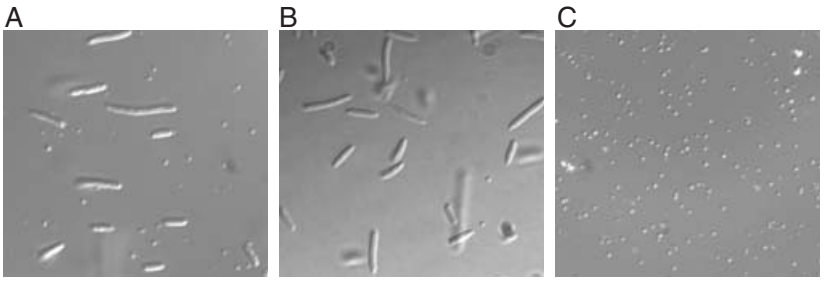

Fig. 1. Representative DIC images showing the separation of rod cells and minicells from the *E. coli* minicell mutant X-1488. Minicell mutant X-1488 (A) was grown in LB broth at 37°C. Rod (B) and minicells (C) isolated by differential centrifugation were examined for their morphology and purity. The cells were viewed under a 100× objective, and images were captured with a CCD camera.

We carried out one-dimensional SDS–PAGE analysis of the membrane proteins isolated from minicells and rod cells to determine whether visual differences in the resulting protein bands were apparent. Equal amounts of membrane proteins from each membrane extract were resolved on 12% glycine–SDS–PAGE and stained by Coomassie blue G-250 or silver. We consistently observed differences in specific membrane protein bands between minicells and rod cells by either Coomassie blue or silver staining (Fig. 2). Cells grown at 30°C and 37°C showed similar protein profiles (data not shown). Interestingly, there were staining variations between different staining dyes. For example, a heavily stained 37–38 kDa protein band was visualized by Coomassie blue but appears as a ghost band (negative staining) when the gel was silver stained (Fig. 2). The reason for this negative staining is not known. From these gels, it is clear that there are subtle differences in the protein profiles of minicell and rod cell membranes.

Comparison of two-dimensional membrane protein profiles between minicells and rod cells

In order to assign protein identities unambiguously to the differentially distributed proteins, we used high-resolution two-dimensional gel electrophoresis to separate membrane proteins and used mass spectrometry (MS) to identify the protein spots. We initially used either broad-range immobilized pH gradient (IPG) strips (pH 3–10) or narrow-range IPG strips (pH 4–7). We found that pH 4–7 IPG strips resolved many of the *E. coli* membrane proteins and gave a better separation of membrane proteins than pH 3–10 IPG strips (data not shown). Hence, pH 4–7 IPG strips were chosen for isoelectric focusing in the experiments described in this paper. For each independent experiment, duplicate analytical gels and one preparative gel were generated for both rod cell and minicell membrane samples obtained from the same cell cultures. To obtain comparable silver-stained protein spots between different gels, the gels used for comparison were stained in the same trays, developed in parallel and digitized as tagged image files (TIF) immediately after staining. Two-dimensional membrane protein profiles from five pairs of silver-stained analytical gels from four independent experiments (from cells grown at 37°C) were compared. Representative examples of unannotated, silver-stained minicell (Fig. 3A) and rod cell (Fig. 3B) membrane samples are shown. By visual comparison, several spots were consistently seen to be enriched in either minicells or rod cells. However, the intensity of some spots varied between experiments.

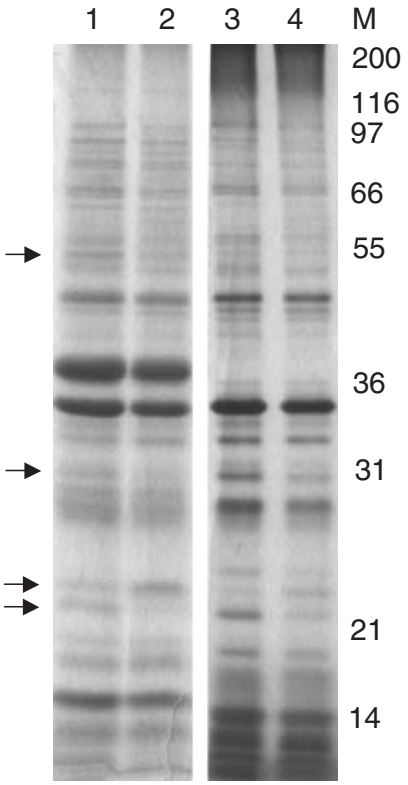

Fig. 2. Membrane protein profiles of rod cells and minicells. Carbonate-washed membrane proteins from rod cells and minicells were separated using 12% glycine-SDS–PAGE. Aliquots of 25 μg of proteins from rod-shaped cells (lane 1) and minicells (lane 2) were loaded on gels stained with Coomassie blue G-250. For gels stained with silver, 5 μg of protein from rod-shaped cells (lane 3) and minicells (lane 4) was loaded. The sizes of molecular weight standards (M) (Novex unstained marker, Invitrogen) are indicated on the right in kDa. Arrows indicate differentially enriched bands. For this experiment, the *E. coli* minicell mutant X-1488 was grown at 37°C.

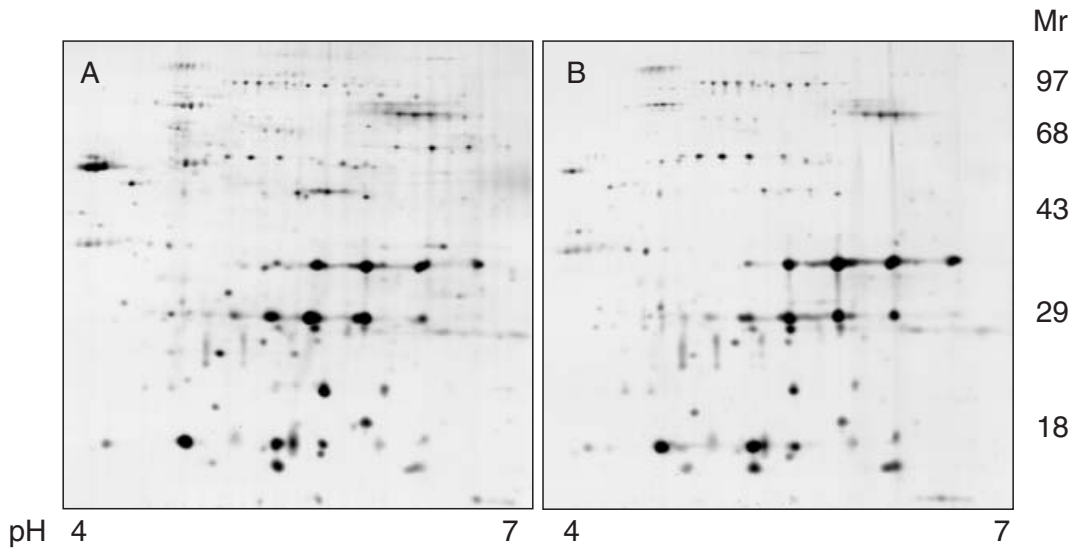

Fig. 3. Two-dimensional gels of carbonate-insoluble membrane proteins from minicells (A) and rod cells (B) fractionated using pH 4–7 IPG strips followed by 11% SDS–PAGE. Samples of 50 μg of protein were loaded on each gel. Proteins were stained with silver. The pH range is shown at the bottom, and the sizes of molecular weight standards (Mr) (Gibco prestained markers) are indicated on the right in kDa.

Comparative overlays of two-dimensional images

To obtain an unbiased assessment of differentially distributed membrane proteins, Z3 two-dimensional analysis software was used as explained in *Experimental procedures*. This analysis program allows for the quantitative comparison of protein spots while adjusting for experimental variations caused by problems such as uneven protein loading or staining variations. To align the gels, the alignment algorithm for spot matching was used. Each gel pair from the same independent experimental set was compared. Spots detected in at least two pairs of gels (from a total of five gel pairs) were used for composite comparison. A representative alignment is shown in Fig. 4. A total of 173 spots were numbered and analysed. Protein identities of 54 spots were obtained (Table 1). The fold enrichment, or differential enrichment value (DE), was obtained for the corresponding spot pairs. The majority of the spots were found to be equally represented in both minicell and rod cell membrane preparations, consistent with the one-dimensional profiles of these membrane proteins (Fig. 2). Interestingly, 36 spots were consistently enriched in minicell membranes (DE value >1) (Table 2), and 15 spots were more abundant in rod cell membranes (DE value <1) (Table 3). These protein spots may represent proteins that are asymmetrically distributed in the *E. coli* cell.

Protein identification by peptide mass fingerprinting (PMF)

To identify these differentially distributed membrane proteins, protein spots of interest, as well as landmark proteins (Molloy *et al*., 2000), were cut out of both analytical and preparative gels and examined by peptide mass fingerprinting (PMF) (Table 1). We mostly identified known or putative outer membrane proteins, a few inner membrane proteins and periplasmic proteins. No cytoplasmic proteins were identified, indicating that the alkaline carbonate treatment efficiently stripped out contaminating soluble proteins. The representation of proteins that we resolved in these experiments is similar to that of other studies of membrane proteins of *E. coli* (Molloy *et al*., 2000) and *C. crescentus* (Phadke *et al*., 2001; Molloy *et al*., 2002).

The predicted mass/pI of each identified protein or precursor (P) was obtained directly from the SWISSPROT database (http://c.expasy.org/sprot). For membrane proteins with putative or known N-terminal signal peptides, we calculated the mass/pI of the putative mature protein (M) using the COMPUTE pI/Mw tool (http://c.expasy.org/tools/pi_tool.html). For hypothetical proteins without known or putative signal peptide, we predicted their cellular localization and signal peptides using SIGNALP (http://www.cbs.dtu.dk/services/SignalP/) or PSORT (http://psort.nibb.ac.jp/).

The characteristics of several proteins identified in this study are noteworthy. The hypothetical proteins YiaF, YfiO and YfgL identified in this study are new gel IDs that have not yet been reported for their expression from previous studies on *E. coli* two-dimensional membrane proteomes (Link *et al*., 1997; Molloy *et al*., 2000). YfgL (spots 87 and 88), YaeC (spot 126) and YfiO (spot 138) are predicted to possess signal peptides and are potential lipoproteins associated with either the inner or the outer membrane

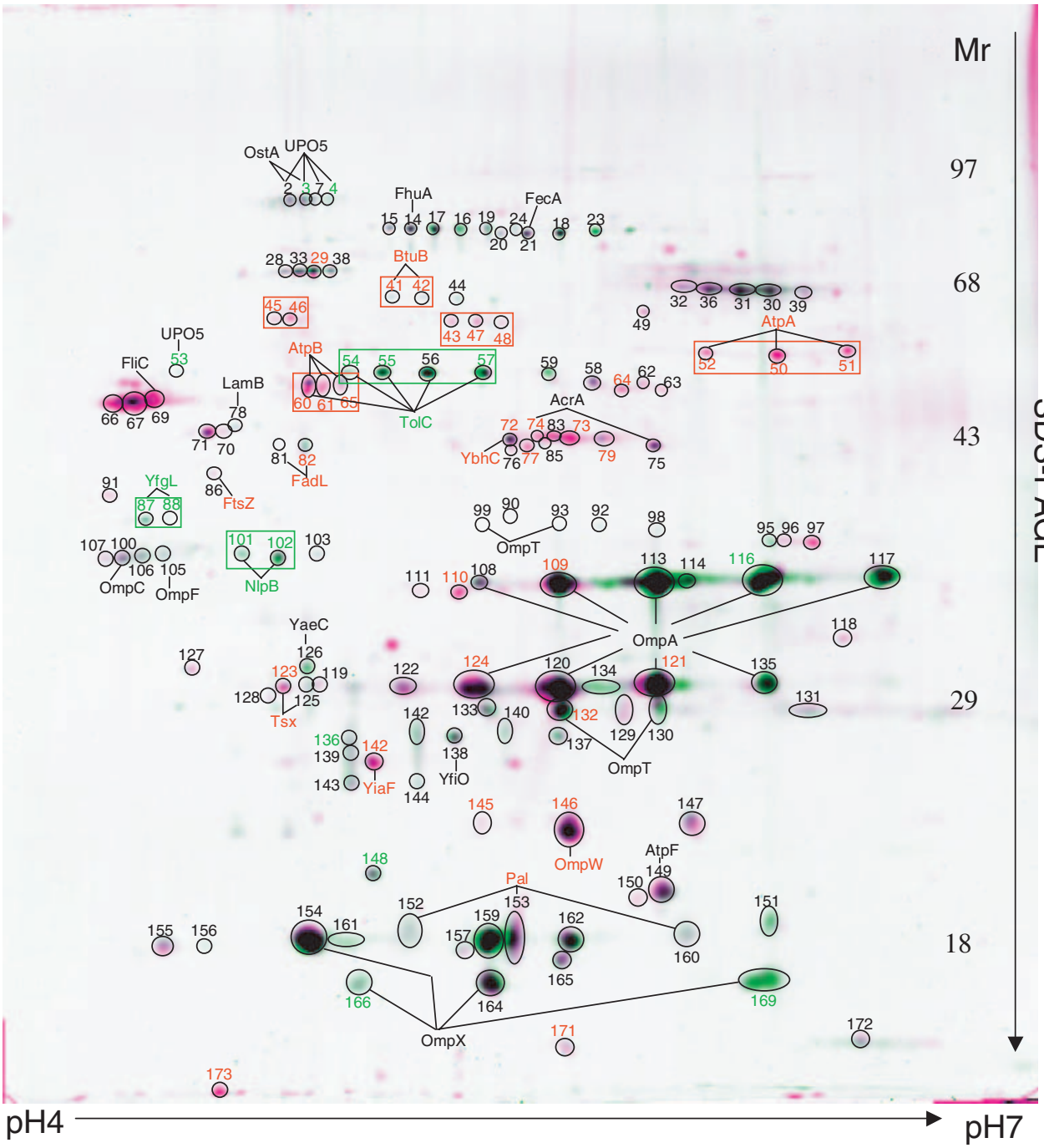

Fig. 4. Composite image showing known proteins and unidentified protein spots that are differentially enriched in minicells and rod cells. Two-dimensional gels from membrane proteins isolated from rod-shaped cells and minicells were digitized and analysed using the Z3 2D image analysis software as described in *Experimental procedures*. A representative image obtained by overlaying two-dimensional gels of rod-shaped (green) and minicell membrane proteins (purple) is shown. The numbers correspond to proteins subjected to MALDI mass fingerprinting, and spots identified in this study are labelled with the protein name. Minicell membrane-enriched spots are labelled in pink, and the spots present more abundantly in rod cell membranes are indicated in green. Protein spots that migrated in chains and were consistently enriched in minicell or rod cell membranes are highlighted in a box. The pH range is shown at the bottom, and the sizes of molecular weight standards (Mr) (Gibco prestained markers, Invitrogen) are indicated on the right in kDa.

Table 1. Identified *E. coli* membrane protein spots by peptide mass fingerprinting.

Spot no.	Accession name	Accession no.	Mowse[a] score	Peptide matched (% coverage)	Signal peptide[b]	Predicted mass/pI (P) mass/pI (M)[c]	Cellular location[d]	Note[e]
2	UPO5_ECOLI	P39170	1.37e + 03	7 (11%)	Y, 1–20	90553.5/4.93 (P) 88426.1/4.87 (M)	Integral OMP	B(1)
2	OSTA_ECOLI	P31554	974	7 (13%)	Y, 1–24	89671.9/4.94 (P) 87068.9/4.85 (M)	Periplasmic	B(1)
3	UPO5_ECOLI	P39170	1.93e + 09	19 (29%)	Y, 1–20	90553.5/4.93 (P) 88426.1/4.87 (M)	Integral OMP	B(1)
3	OSTA_ECOLI	P31554	3.37e + 06	12 (23%)	Y, 1–24	89671.9/4.94 (P) 87068.9/4.85 (M)	Periplasmic	B(1)
4	UPO5_ECOLI	P39170	5.07e + 03	10 (12%)	Y, 1–20	90553.5/4.93 (P) 88426.1/4.87 (M)	Integral OMP	B(1)
7	UPO5_ECOLI	P39170	8.41e + 05	14 (18%)	Y, 1–20	90553.5/4.93 (P) 88426.1/4.87 (M)	Integral OMP	B(2) S(1)
14	FHUA_ECOLI	P06971	5.11e + 07	15 (27%)	Y, 1–33	82182.7/5.47 (P) 78742.1/5.13 (M)	Integral OMP	B(1) S(1)
21	FECA_ECOLI	P13036	7.52e + 06	14 (23%)	Y, 1–33	85322.0 5.53 (P) 81707.2/5.36 (M)	Integral OMP	B(1) S(1)
41	BTUB_ECOLI	P06129	3.44e + 03	10 (37%)	Y, 1–20	68407.6/5.23 (P) 66325.6/5.10 (M)	Integral OMP	B(1) 200 p.p.m.
42	BTUB_ECOLI	P06129	1.82e + 10	18 (42%)	Y, 1–20	68407.6/5.23 (P) 66325.6/5.10 (M)	Integral OMP	B(2) S(1)
50	ATPA_ECOLI	P00822	1.56e + 04	8 (21%)	N	55222.5/5.80	Associated IMP	B(2) S(1)
51	ATPA_ECOLI	P00822	9.5e + 05	13 (35%)	N	55222.5/5.80	Associated IMP	B(1)
52	ATPA_ECOLI	P00822	3.19e + 05	13 (34%)	N	55222.5/5.80	Associated IMP	B(1)
53	UPO5_ECOLI	P39170	2.97e + 07	15 (24%)	Y, 1–20	90553.5/4.93 (P) 88426.1/4.87 (M)	Integral OMP	B(2), truncated C-terminal domain
54	TOLC_ECOLI	P02930	151	5 (12%)	Y, 1–24	54014.5/5.46 (P) 51468.9/5.23 (M)	Integral OMP	B(1)
55	TOLC_ECOLI	P02930	1.24e + 03	6 (14%)	Y, 1–24	54014.5/5.46 (P) 51468.9/5.23 (M)	Integral OMP	B(1)
56	TOLC_ECOLI	P02930	1.13e + 06	12 (27%)	Y, 1–24	54014.5/5.46 (P) 51468.9/5.23 (M)	Integral OMP	B(2) S(1)
57	TOLC_ECOLI	P02930	4.78e + 04	9 (23%)	Y, 1–24	54014.5/5.46 (P) 51468.9/5.23 (M)	Integral OMP	B(1)
60	TOLC_ECOLI	P02930	1.31e + 04	10 (21%)	Y, 1–24	54014.5/5.46 (P) 51468.9/5.23 (M)	Integral OMP	B(2) S(1)
60	ATPB_ECOLI	P00824	1.98e + 08	16 (42%)	N	50325.9/4.90	Associated IMP	B(1)
61	ATPB_ECOLI	P00824	1.19e + 08	16 (44%)	N	50325.9/4.90	Associated IMP	B(1)
65	ATPB_ECOLI	P00824	1.1e + 10	18 (54%)	N	50325.9/4.90	Associated IMP	B(1)
69	FLIC_ECOLI	P04949	7.44e + 04	8 (26%)	N	51295.2/4.50	Flagella	B(1) S(1)
72	YBHC_ECOLI	P46130	1.24e + 06	10 (31%)	Y, 1–21	46082.6/5.66 (P) 43916.6/5.49 (M)	OM lipoprotein	B(2) S(1)
74	ACRA_ECOLI	P31223	2.92e + 04	7 (33%)	Y, 1–24	42197.0/7.69 (P) 39723.7/6.08 (M)	IM lipoprotein	B(1)
75	ACRA_ECOLI	P31223	71.8	3 (10%)	Y, 1–24	42197.0/7.69 (P) 39723.7/6.08 (M)	IM lipoprotein	B(1)
78	LAMB_ECOLI	P02943	9.81e + 04	10 (32%)	Y, 1–25	49912.5/4.81 (P) 47385.0/4.72 (M)	Integral OMP	B(1)
81	FADL_ECOLI	P10384	1.61e + 05	9 (26%)	Y, 1–27	48857.4/5.19 (P) 45991.5/4.99 (M)	Integral OMP	B(1)
82	FADL_ECOLI	P10384	3.76e + 04	8 (23%)	Y, 1–27	48857.4/5.19 (P) 45991.5/4.99 (M)	Integral OMP	B(1) 300 p.p.m.
86	FTSZ_ECOLI	P06138	4.08e + 09	16 (57%)	N	40297.3/4.72	Cytoplasmic, associated with IM	B(1)
87	YFGL_ECOLI	P77774	2.05e + 04	7 (28%)	Y, 1–24 SignalP	41887.5/4.72 (P) 39287.9/4.61 (M)	IM or OM lipoprotein PSORT	B(1)
88	YFGL_ECOLI	P77774	1.88e + 06	12 (41%)	Y, 1–24 SignalP	41887.5/4.72 (P) 39287.9/4.61 (M)	IM or OM lipoprotein PSORT	B(1)
93	OMPT_ECOLI	P09169	2.43e + 03	7 (25)	Y, 1–20	35562.5/5.76 (P) 33477.7/5.38 (M)	Integral OMP	B(1) S(1)
99	OMPT_ECOLI	P09169	2.27e + 05	11 (41%)	Y, 1–20	35562.5/5.76 (P) 33477.7/5.38 (M)	Integral OMP	B(1) S(1)
100	OMPC_ECOLI	P06996	9.42e + 03	6 (24%)	Y, 1–21	40368.3/4.58 (P) 38307.5/4.48 (M)	Integral OMP	B(1) S(1)
101	NLPB_ECOLI	P21167	5.13e + 04	8 (29%)	Y, 1–24	36842.7/5.34 (P) 34371.3/4.96 (M)	OM lipoprotein	B(2)

Table 1. *cont.*

Spot no.	Accession name	Accession no.	Mowse[a] score	Peptide matched (% coverage)	Signal peptide[b]	Predicted mass/pI (P) mass/pI (M)[c]	Cellular location[d]	Note[e]
102	NLPB_ECOLI	P21167	1.72e + 06	11 (40%)	Y, 1–24	36842.7/5.34 (P) 34371.3/4.96 (M)	OM lipoprotein	B(2)
105	OMPF_ECOLI	P02931	184	3 (14%)	Y, 1–22	39333.5/4.76 (P) 37084.5/4.64 (M)	Integral OMP	B(1)
108	OMPA_ECOLI	P02934	7.08e + 03	7 (24%)	Y, 1–21	37200.9/5.99 (P) 35172.3/5.26 (M)	Integral OMP	B(1)
113	OMPA_ECOLI	P02934	1.73e + 03	10 (23%)	Y, 1–21	37200.9/5.99 (P) 35172.3/5.26 (M)	Integral OMP	B(1) S(1)
116	OMPA_ECOLI	P02934	6.08e + 04	10 (32%)	Y, 1–21	37200.9/5.99 (P) 35172.3/5.26 (M)	Integral OMP	B(1) S(1)
117	OMPA_ECOLI	P02934	841	5 (21%)	Y, 1–21	37200.9/5.99 (P) 35172.3/5.26 (M)	Integral OMP	B(1) S(1)
120	OMPA_ECOLI	P02934	2.32e + 03	6 (24%)	Y, 1–21	37200.9/5.99 (P) 35172.3/5.26 (M)	Integral OMP	B(1) S(1)
121	OMPA_ECOLI	P02934	6.47e + 04	10 (32%)	Y, 1–21	37200.9/5.99 (P) 35172.3/5.26 (M)	Integral OMP	B(1) S(1)
123	TSX_ECOLI	P22786	6.02e + 03	6 (26%)	Y, 1–22	33589.3/5.07 (P) 31413.4/4.87 (M)	Integral OMP	B(1)
125	TSX_ECOLI	P22786	3.09e + 03	5 (29%)	Y, 1–22	33589.3/5.07 (P) 31413.4/4.87 (M)	Integral OMP	B(3) S(1)
126	YAEC_ECOLI	P28635	1.98E + 04	7 (39%)	Y, 1–22	29431.6/5.13 (P) 27236.9/4.93 (M)	IM or OM lipoprotein PSORT	B(1) S(1)
130	OMPT_ECOLI	P09169	2.07e + 04	9 (31%)	Y, 1–20	35562.5/5.76 (P) 33477.7/5.38 (M)	Integral OMP	B(1)
132	OMPT_ECOLI	P09169	3.47e + 04	10 (37%)	Y, 1–20	35562.5/5.76 (P) 33477.7/5.38 (M)	Integral OMP	B(2) S(1)
138	YFIO_ECOLI	P77146	2.82e + 04	10 (38%)	Y, 1–19	27829.5/6.16 (P) 25789.9/5.48 (M)	IM or OM lipoprotein PSORT	B(1)
142	YIAF_ECOLI	P37667	4.01e + 03	5 (21%)	Y, 1–42 (Psort) Y, 1–65 (SignalP)	30158.8/9.36 (P) 25460.8/6.06 (M) (Psort) 23083.9/5.27 (M) (SignalP)	IMP	B(2) S(1)
146	OMPW_ECOLI	P21364	2.67e + 03	4 (40%)	Y, 1–21	22927.9/6.03 (P) 20852.3/5.59 (M)	Integral OMP	B(3) S(2)
149	ATPF_ECOLI	P00859	270	6 (28%)	N	17264.0/5.99	Associated IMP	B(1)
153	PAL_ECOLI	P07176	1.19e + 04	7 (53%)	Y, 1–21	18824.3/6.29 (P) 16616.3/5.59 (M)	OM lipoprotein	B(1) S(1)
154	OMPX_ECOLI	P36546	2.01e + 03	5 (40%)	Y, 1–23	18602.7/6.56 (P) 16382.9/5.30 (M)	Integral OMP	S(2)
164	OMPX_ECOLI	P36546	1.75e + 04	6 (43%)	Y, 1–23	18602.7/6.56 (P) 16382.9/5.30 (M)	Integral OMP	B(1)
166	OMPX_ECOLI	P36546	736	4 (31%)	Y, 1–23	18602.7/6.56 (P) 16382.9/5.30 (M)	Integral OMP	B(1) 300 p.p.m.
169	OMPX_ECOLI	P36546	4.96e + 04	8 (49%)	Y, 1–23	18602.7/6.56 (P) 16382.9/5.30 (M)	Integral OMP	B(2) 300 p.p.m.

a. Molecular Weight Search Score (Pappin *et al*., 1993).
b and **d.** The presence (Y, the length of signal peptide is shown) or absence (N) of signal peptides and cellular location was indicated according to SWISSPROT database information. Some proteins without known topology were analysed further by PSORT or SIGNALP for prediction of possible signal peptides and cellular location in this study. IM indicates inner membrane and OM indicates outer membrane.
c. P, precursor without cleavage of signal peptide; M, mature protein after cleavage of signal peptide.
e. The protein IDs were identified from Coomassie blue-stained gel (B) and/or silver-stained gel (S). The number of times the spots were identified is indicated in parenthesis. A mass accuracy of 150 p.p.m. was used as cut-off for PMF search except in some cases as indicated.

(Table 1 and Fig. 4). YiaF (spot 142, Table 1) is a putative inner membrane protein predicted to have a signal peptide at amino acids 1–42 or 1–65, as predicted by PSORT or SIGNALP respectively. YiaF migration on the two-dimensional gels was consistent with a protein having a mass/pI of 23083.9/5.27, which corresponds to the first 65 N-terminal residues being removed. However, the detection of an m/z peak matching the 50R–69E peptide suggests that the cleavage site is between amino acid residues 42 and 43. The annotated *yiaF* open reading frame (ORF) appears to be correct as examined by ORF FINDER. Thus, it appears that this protein migrates anomalously on our gels. Although the majority of the proteins migrated at positions matching their predicted mass/pI,

Table 2. Protein spots enriched in minicell membranes.

Spot no.	DE[a], Average (lowest, highest) values	Spots with DE > 1/ total spots detected	Protein ID
29	1.5 (1.29, 1.98)	3/3	NA
41	1.66 (1.19, 1.98)	4/4	BTUB
42	2.33 (1.55, 5.06)	3/5	BTUB
43	Min only[b]	4/4	NA
45	Min only	3/3	NA
46	4.74 or Min only	3/3	NA
47	5.38	4/4	NA
48	Min only	3/3	NA
50	2.28 (1.26, 2.68)	5/5	ATPA
51	7.36 (2.05, 12.66)	3/3	ATPA
52	2.74 or Min only	3/3	ATPA
58	1.84 (1.53, 2.29)	3/3	NA
60	2.15 (1.31, 2.85)	5/5	ATPB and TOLC
61	3.27 or Min only	3/3	ATPB
64	4.62 (1.68, 7.55)	4/4	NA
65	2.58 (2.16, 3.46)	5/5	ATPB
72	1.49 (1.19, 2.34)	5/5	YBHC
73	2.53 or Min only	4/4	NA
74	Min only	4/4	ACRA
77	Min only	3/3	NA
79	3.12 (1.60, 4.10)	4/4	NA
82	3.03 (1.06, 4.90)	4/5	FADL
86	3.28 (2.64, 4.39)	3/4	FtsZ
109	1.84 (1.18, 3.66)	4/5	OMPA
110	5.68 (1.65, 13.68)	3/3	NA
121	1.41 (1.1, 1.75)	4/5	OMPA
123	2.30 (1.1, 5.25)	5/5	TSX
124	1.93 (1.33, 2.52)	4/5	OMPA
132	1.29 (1.20, 1.43)	4/5	OMPT
142	2.82 (1.64, 6.25)	5/5	YIAF
145	2.59 or Min only	5/5	NA
146	1.46 (1.31, 1.72)	3/5	OMPW
153	2.43 (1.21, 7.10)	5/5	PAL
168	1.23 or Min only	3/3	NA
171	2.64 (1.69, 3.58)	4/4	NA
173	Min only	3/3	NA

a. DE is the differential enrichment value from minicells versus rod cells; only the value >1 is included for average value.
NA, data not available.
b. Min only, spots detected in minicells only.

several proteins, such as UPO5, BtuB, AtpA, AtpB, FadL, YfgL, Tsx and Pal, resolved as two or more spots of similar mass but different isoelectric points (Fig. 4). These may represent natural isoforms or an artifact caused by sample preparation or two-dimensional electrophoresis. Similarly, several proteins, such as TolC, AcrA, NlpB, OmpA, OmpT and OmpX, resolved in multiple spots of differing masses and pIs, suggesting possible protein processing, degradation and/or modifications (Fig. 4). Similar migration for several of these proteins has been observed previously (Molloy *et al*., 2000).

Summary of the identified differentially distributed membrane proteins

We successfully identified the proteins in 20 out of 36 minicell-enriched spots and found 13 unique proteins (Table 2). Among this class was the septal protein FtsZ (spot 86, Table 2). Even though FtsZ is a peripheral membrane protein, it is the most abundant of all cell division proteins totalling 10–20 thousand copies per *E. coli* cell (Bi *et al*., 1991). Thus, although we included a sodium carbonate wash step that removes peripheral membrane proteins, the abundance of FtsZ could have resulted in its retention in rod cell and minicell membrane protein preparations. Because the ratio of division septa to total membrane in minicells is higher than in rod cells, it is reasonable to detect more FtsZ in minicells. With the exception of FtsA (the relative stoichiometry of which compared with FtsZ is 1:150), the other cell division proteins ZipA, FtsW, FtsK, FtsL, FtsN, FtsI and FtsQ are membrane proteins (Errington *et al*., 2003). Their relatively low abundance combined with the technical difficulty in focusing inner membrane proteins on IPG strips may have prevented their detection in our study.

YbhC (putative pectinesterase lipoprotein), YiaF (hypothetical inner membrane protein) and OmpW (colicin receptor) migrate as single spots on two-dimensional gels with average minicell biases of 1.49, 2.82 and 1.46 respectively (Fig. 4 and Table 2). Thus, these proteins are strong candidates for polar or septal proteins. Several proteins were found in multiple spots with one or more spots biased to the minicell membrane preparations. Although BtuB (Vitamin B12 receptor), AtpA and AtpB (α and β subunits of F_0F_1 ATP synthase) migrate as multiple spots on two-dimensional gels, all the spots identified have DE values >1 (Fig. 4 and Table 2), consistent with a minicell bias for these proteins. AcrA (a component of a multidrug efflux pump) was detected as two spots (74 and 75), one of which was only present in minicells (spot 74, Table 2), whereas the other was equally distributed in both cell types (Fig. 4). FadL (long-chain fatty acid transport protein) also migrated as two spots (81 and 82, Fig. 4),

Table 3. Protein spots enriched in rod cell membranes.

Spot no.	DE[a], Average (lowest, highest) values	Spots with DE > 1/ total spots detected	Protein ID
3	0.63 (0.36, 0.85)	4/5	UPO5, OSTA
4	0.43 (0.24, 0.77)	3/3	UPO5
53	0.35 (0.28, 0.42)	3/3	UPO5
54	0.56 (0.24, 0.72)	3/5	TOLC
55	0.77 (0.40, 0.94)	4/5	TOLC
57	0.54 (0.22, 0.75)	3/3	TOLC
87	0.60 (0.25, 0.86)	4/4	YFGL
88	0.70 (0.56, 0.87)	5/5	YFGL
101	0.54 (0.31, 0.82)	4/5	NLPB
102	0.67 (0.47, 0.84)	5/5	NLPB
116	0.77 (0.75, 0.79)	4/5	OMPA
136	0.55 (0.24, 0.87)	4/5	NA
148	0.65 (0.47, 0.75)	4/5	NA
166	0.36 (0.20, 0.51)	3/3	OMPX
169	0.66 (0.41, 0.90)	3/3	OMPX

a. DE is the differential enrichment value of minicells versus rod cells; only the value <1 is included for average value.
NA, data not available.

and there was a strong minicell bias with the more abundant spot (82, Table 2). Therefore, we include FadL and AcrA as polar protein candidates. Similarly, although OmpT (outer membrane protease), Tsx (outer membrane channel-forming protein) and Pal (group A colicin uptake) migrated as multiple isoforms (4, 2 and 3 respectively), in each case, the more abundant protein spot (132, 123 and 153 respectively) was enriched in minicell membranes (Fig. 4 and Table 2). Thus, determining the localization of these proteins is warranted. Finally, several additional spots (45, 46, 43, 47, 48, and 145) were often detected only from minicell membranes; we were unable to obtain the protein identities by PMF, perhaps because of low protein concentration.

We also identified 13 of the 15 spots enriched in rod cells and found seven unique proteins. Both isoforms of NlpB (putative lipoprotein) and YfgL (putative lipoprotein) as well as three isoforms of UPO5 (hypothetical outer membrane protein) were enriched in rod cell membranes (Fig. 4 and Table 3). Although OstA (a protein involved in outer membrane biogenesis) co-migrates with an isoform of UPO5, it was not detected in minicells and may be rod cell biased as well (Fig. 4 and Table 3). OmpX migrates as multiple isoforms (Fig. 4), and two of the minor forms are enriched in rod cell membranes (Table 3); therefore, the majority of OmpX protein is distributed evenly in the two cell types.

Two proteins are of particular interest, as they possess isoforms enriched in minicells and in rod cells. OmpA migrates at predominantly two different molecular weights each with multiple isoforms (Fig. 4). Three of these spots (109, 124 and 121) are enriched in minicells (Table 2), one spot (116) enriched in rod cells (Table 3), and the remaining five spots (108, 113, 117, 120 and 135) are equally distributed. TolC migrates at two distinct molecular weights. Three of the more slowly migrating isoforms (spots 54, 55 and 57) are enriched in rod cells (Table 3), whereas a fourth spot (56) is equally distributed. A slightly faster migrating isoform (spot 60, Table 2) may be enriched in minicells. Spot 60 also contains AtpB, and the relative contribution to the spot intensity by TolC and AtpB could not be determined in this study (Table 1). Regardless, it is of interest that these multiple isoforms are differentially enriched in the cell preparations.

Immunoblot analysis of selective membrane proteins

We have shown previously that the inner membrane MCPs are clustered predominantly at the poles and, therefore, these proteins are ideal candidates to test whether minicells are enriched for polar proteins. Unfortunately, in general, inner membrane proteins do not resolve well on two-dimensional gels because of their inability to focus in the first dimension (Molloy, 2000). Consistent with this, we did not detect MCPs on our two-dimensional gels. To determine whether MCPs were enriched in minicells, equal amounts of membrane proteins prepared from either rod cell or minicell membranes from cells grown at 30°C or 37°C were fractionated on one-dimensional gels and analysed by immunoblotting using antibodies against MCPs. Quantification of MCP signal reveals that the amount of these proteins is 1.5-fold greater in minicell membranes from cells grown at 37°C (Fig. 5) and fivefold enhanced in minicell membranes at 30°C (optimum temperature for MCP expression) (Fig. 5). We next examined the distribution of the total protein for several proteins that had multiple isoforms on two-dimensional gels and in which one or more isoforms were enriched in minicells or rod cells. The majority of the isoforms of TolC were enriched in rod cells (Fig. 4 and Table 3). Consistent with this, we found a three- to four-fold enrichment of TolC in rod cell extracts (Fig. 5). OmpA has many isoforms with differing levels of abundance in the two membrane preparations (Fig. 4, Tables 1, 2 and 3). Total OmpA is distributed equally between the two cell types (Fig. 5). In addition, as only one band is detected by one-dimensional gel, the different-sized isoforms of OmpA seen on the two-dimensional gels are likely to

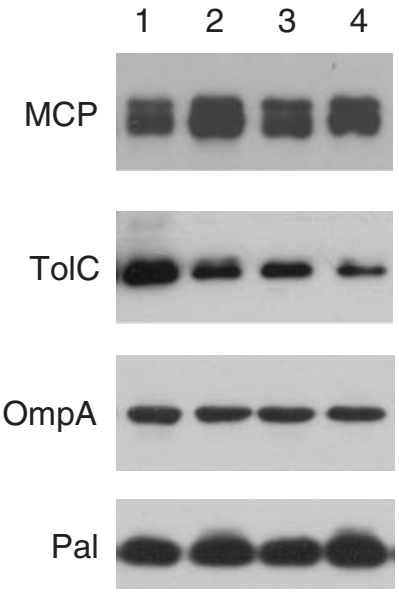

Fig. 5. Immunoblot analysis showing expression patterns of MCPs, TolC, OmpA and Pal in rod and minicell membranes. Carbonate-washed membrane proteins were fractionated on glycine–SDS–PAGE followed by immunoblot analysis as described in *Experimental procedures*. Samples of 2.5 μg of membrane protein were loaded in each lane. Membrane proteins from rod cells are loaded in lanes 1 and 3. Lanes 2 and 4 show membrane proteins from minicells. Cells were grown at 30°C for samples shown in lanes 1 and 2 and at 37°C for samples shown in lanes 3 and 4. Antisera used for immunoblot analysis are indicated on the left. The signals were quantified using a Fluor-S MAX MultiImager (Bio-Rad). Shown here are results from one of two independent experiments.

result from modification that occurred during two-dimensional electrophoresis. Finally, we examined the distribution of the total levels of Pal, a protein with multiple isoforms, one of which (spot 153) is enriched on two-dimensional gels of minicell membrane extracts (Fig. 4 and Table 2). Consistently, on one-dimensional gels, total Pal is slightly enriched (1.2-fold) in minicell extracts at either 30°C or 37°C (Fig. 5).

Localization of epitope-tagged OmpW and YiaF by immunofluorescence microscopy

To determine whether the minicell-enriched membrane proteins that we identified in this study were preferentially distributed to the end of cell, we determined the localization of two polar candidates, OmpW and YiaF. OmpW and YiaF were C-terminally fused to haemagglutinin (HA) and FLAG epitope tags, respectively, and expressed under the control of their native promoters on plasmids or on the chromosome. The localization of OmpW and YiaF was determined by immunofluorescence using antisera against these tags. Approximately 35% of the cells containing OmpW-HA on a low-copy plasmid expressed detectable levels of the fusion protein (data not shown). In these cells, OmpW-HA localized predominantly to the cell poles (Fig. 6A), whereas the immunostaining of the remaining cells was comparable to background signal (no primary antibody or cells lacking the OmpW-HA clone; data not shown). We did not detect expression of chromosomally tagged OmpW-HA (data not shown).

YiaF-FLAG was not randomly distributed around the inner membrane but had a patchy localization (Fig. 6B). Although patches of fluorescence could be observed along the lateral edges, the majority of the signal was at the poles. In dividing cells, YiaF-FLAG was often localized to the division septum. We observed similar expression and localization patterns for YiaF-FLAG expressed from either the chromosome or a medium-copy plasmid. No staining was obtained when either no primary antibody was used or cells lacking the epitope tags were stained with both primary and secondary antisera (data not shown).

In contrast to the non-random localization patterns of the minicell-enriched OmpW and YiaF proteins, OmpA, a protein found in both minicells and rod cells, was randomly distributed in the cell membrane (Fig. 6C). In this case, we localized OmpA with anti-OmpA antibodies. Taken together, these data suggest that our proteomic analysis of minicell proteins is biologically relevant in the context of protein localization.

Discussion

In this study, we used proteomic analysis systematically to identify polar membrane proteins. We have identified at least 12 proteins that are differentially enriched in minicells versus rod cell membranes (Table 4). Previous analyses of the protein composition of *E. coli* minicells have led to conflicting conclusions as to whether proteins were preferentially biased to either minicells or rod cells. In

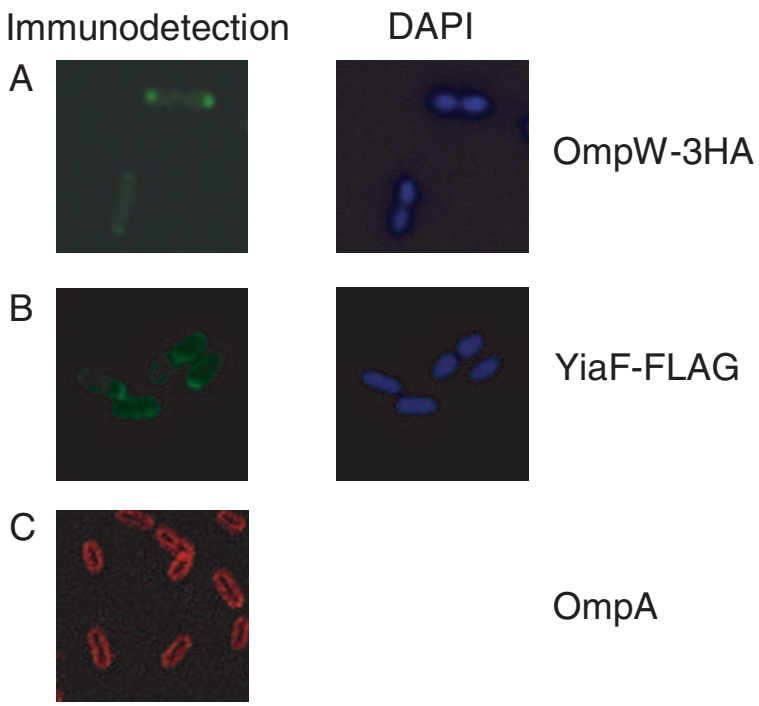

Fig. 6. Localization patterns of OmpW-HA, YiaF-Flag and OmpA.DH5α cells expressing OmpW-HA and OmpA were used for immunolocalization of OmpW-HA and OmpA. YiaF-FLAG localization was performed in TOP10 cells expressing FLAG epitope-tagged YiaF. Immunofluorescence staining with an anti-HA (primary antibody) and fluorescein-labelled goat anti-rabbit antiserum (secondary antibody) reveals polar OmpW-HA signals (A). Patchy distribution of YiaF-FLAG with polar and septal foci (B) is seen by immunostaining with anti-FLAG (primary antibody) and fluorescein-labelled goat anti-mouse antiserum (secondary antibody). Random, membrane-associated distribution of OmpA (C) is seen using anti-OmpA (primary antibody) and fluorescein-labelled goat anti-mouse antiserum (secondary antibody).

Table 4. Known or putative function of the identified differentially distributed membrane proteins.

Protein name	Differentially enriched compartment	Evidence for differential distribution	Known or putative function and localization
MCP	Minicell	Immunoblot analysis	Chemoreceptors, IM
AtpA	Minicell	2-DE comparison	F_0F_1 ATP synthase α subunit, IM
AtpB	Minicell	2-DE comparison	F_0F_1 ATP synthase β subunit, IM
YbhC	Minicell	2-DE comparison	Hypothetical lipoprotein, pectinesterase family, OM
Tsx	Minicell	2-DE comparison	Colicin K and phage T6 receptor, channel for nucleosides, OM
YiaF	Minicell	2-DE comparison	Hypothetical novel protein, IM
OmpW	Minicell	2-DE comparison	Putative colicin S4 receptor, OM
Pal	Minicell	2-DE comparison Immunoblot analysis	Putative lipoprotein, colicin import, membrane integrity
BtuB	Minicell	2-DE comparison	Vitamin B12 receptor, OM
FtsZ	Minicell	2-DE comparison	Z-ring subunit at cell division sites, IM and cytoplasmic
AcrA	Minicell	2-DE comparison	Component of a multidrug efflux pump, putative IM lipoprotein
FadL	Minicell	2-DE comparison	Long-chain fatty acid transport protein, OM
OmpT	Minicell	2-DE comparison	Outer membrane protease
TolC	Rod-shaped cell	2-DE comparison Immunoblot analysis	Multidrug efflux, protein export, tolerance to colicin, cell division, OM
YfgL	Rod-shaped cell	2-DE comparison	Putative lipoprotein, OM or IM
NlpB	Rod-shaped cell	2-DE comparison	Putative lipoprotein, OM
UPO5	Rod-shaped cell	2-DE comparison	Hypothetical outer membrane protein
OstA	Rod-shaped cell	2-DE comparison	Involved in outer membrane biogenesis, OM

some previous studies, no differences were observed in the protein profiles of these cell types (Wilson and Fox, 1971; Green and Schaechter, 1972; Goodell and Schwarz, 1977). In other studies, however, specific enzyme activities such as alkaline phosphatase, cyclic phosphodiesterase and 5′-nucleotidase, and acid hexose monophosphatase were found to be higher in minicells than in rod cells (Dvorak *et al*., 1970), and these could represent polar localization of the respective proteins.

Immunolocalization of two epitope-tagged minicell-enriched proteins, OmpW and YiaF, reveals that the former shows polar distribution whereas the latter shows a patchy localization pattern with distinct polar and septal foci (Fig. 6). On the other hand, similar studies with OmpA, the amounts of which are equal in minicell and rod cell membranes (Fig. 5), show that this protein is localized throughout the cell membrane (Fig. 6). Thus, the subcellular location of these proteins is in agreement with the results obtained from our proteomics analysis (Table 4). Therefore, it is likely that the other minicell-enriched proteins found in our study are indeed located at the poles in wild-type cells.

Although our study has identified a number of potentially polar membrane proteins, it has not identified all the membrane proteins that are differentially enriched in the two cell types. This may be due to poor expression or lower stability of membrane proteins in a minicell mutant background. Furthermore, it is likely that some membrane proteins are inadequately solubilized under our experimental conditions in spite of using a potent detergent C8ϕ (a sulphobetaine surfactant with *p*-phenyloctyl tail) (Molloy, 2000; Phadke *et al*., 2001; Molloy *et al*., 2002). Nevertheless, we are encouraged by the detection of a significant number of integral outer membrane proteins and a few inner membrane proteins in our study.

We are intrigued to discover two known and two putative lipoproteins that are differentially distributed between minicell and rod cell membrane proteomes (Tables 2 and 3 and Fig. 4). Among these, YbhC and Pal are enriched in minicells while YfgL and NlpB are present more abundantly in rod cell membranes. Pal is an outer membrane-anchored protein that has been shown to bind the major outer membrane proteins Lpp and OmpA and to be important in maintaining the integrity of the outer membrane of *E. coli* (Table 4) (Cascales *et al*., 2002). Although the total Pal is only 1.2-fold enriched in minicell membranes (Fig. 5), one of its isoforms (spot 153, Fig. 4) is enriched in minicells (Table 1), raising the possibility that this isoform of Pal is a polar protein. NlpB (Table 4) has been shown to be an outer membrane lipoprotein, although its function is not clear (Bouvier *et al*., 1991). YbhC and YfgL (Table 4) are putative lipoproteins based on sequence similarity with other known lipoproteins, but their association with lipids has not been established. It has been shown that the anionic membrane phospholipid cardiolipin is enriched in minicells (Koppelman *et al*., 2001) and in the septal and polar regions of wild-type *E. coli* cells (Mileykovskaya and Dowhan, 2000). Taken together, these results suggest that there may indeed be differences in protein and lipid composition that contribute to the different microenvironments of lateral and polar membranes.

AtpA and AtpB are minicell-enriched proteins that resolve as multiple spots on two-dimensional gels

(Tables 1 and 2 and Fig. 4). AtpA and AtpB are α and β subunits of the F_0F_1 ATP synthase complex respectively (Table 4) (Altendorf *et al*., 2000). More specifically, AtpA and AtpB are proteins associated with the extramembranous F_1 component of ATP synthase. It is puzzling that we were able to detect these peripheral membrane proteins enriched in minicells but not proteins of the membrane-embedded F_0 subunit. For example, AtpF, the β subunit of the F_0 component, was not enriched in minicells (Fig. 4, spot 149). One possibility is that the F_1 complex may be more tightly associated with the membrane-embedded F_0 complex in minicells than in rod-shaped cells. Experiments to test this possibility are in progress. We were also unable to detect YidC, which has been shown to be important for the membrane insertion of the α and β subunits of the F_0 sector of the ATP synthase complex (Yi *et al*., 2003). Interestingly, localization studies using a YidC–GFP fusion have shown that this protein is polar (Urbanus *et al*., 2002).

Several porin-like outer membrane proteins, Tsx, OmpW and BtuB, are enriched in minicell membranes (Table 1 and Fig. 4). All three proteins are shown to be colicin receptors (Table 4) (Bremer *et al*., 1990; Pilsl *et al*., 1999). Additionally, Tsx also serves as a channel for nucleoside import (Table 4) (Riede *et al*., 1984; Bremer *et al*., 1990), and BtuB is a receptor required for the binding and uptake of vitamin B12 and bacteriophage BF23 (Table 4) (Gudmundsdottir *et al*., 1988).

YiaF is a hypothetical inner membrane protein with one transmembrane region. Although its function is unknown, YiaF is highly conserved in *E. coli*, *S. flexneri* and *Salmonella enterica*, and it also has orthologues with significant homology in *Y. pestis* and *Pseudomonas syringae* pv. tomato strain DC3000 (data not shown). The disruption of YiaF did not reveal any growth phenotype (A. Henry, U. Nair and J. R. Maddock, unpublished results). Based on PSORT and PMF analysis, we also predict that YaiF has a signal peptide that is 42 amino acids long (Table 1). In our study, YiaF resolved as a single spot and is about threefold more abundant in minicells versus rod cells in all the five gel pairs examined (Table 2). Our data demonstrate that YiaF is a *bona fide* minicell-enriched membrane protein. Surprisingly, it was not identified in a recent, comprehensive proteomic analysis of cell membrane proteins of *E. coli* in which 394 gene products were identified (Fountoulakis and Gasser, 2003).

TolC is a multifunctional outer membrane protein that resolves as multiple isoforms on our two-dimensional gels. The majority of TolC spots are more abundant in rod cell membranes, although one faster migrating spot is enriched in minicell membranes (Table 2 and Fig. 4). An intriguing possibility is that TolC has at least two different isoforms with different spatial localizations. TolC is involved in the production of the peptide antibiotic microcin J25 (Delgado *et al*., 1999), colicin V secretion (Fath *et al*., 1994; Zhang *et al*., 1995), and is also required for maintaining outer membrane integrity (Bernadac *et al*., 1998). In addition to these functions, TolC (also named MukA) functions in chromosome segregation (Hiraga *et al*., 1989; Hiraga *et al*., 1991; Bahloul *et al*., 1996). The localization pattern of TolC remains to be examined.

Our ultimate goal is to understand the factors that contribute to the unique microenvironment of the cell poles. We view this study as an important first step in dissecting the polar microenvironment of the *E. coli* cell and have expanded the list of proteins that exhibit asymmetric subcellular localization. Future challenges include localizing the proteins that we have identified and assessing their roles in maintaining the polarity of other known polar proteins.

Experimental procedures

Separation of minicell and rod cells

The *E. coli* minicell mutant X-1488 (*F⁻ str^r hst⁻ hsm⁺ minA⁻ minB⁻ purE⁻ pdxC⁻ his⁻ ile⁻ met⁻ ade⁻ ura⁻ r⁻ m⁺k*) was used as a source of rod cells and spherical minicells (Meagher *et al*., 1977). Cells (2–3 l) were grown in LB broth (Miller, 1972) at either 37°C (optimal temperature for the growth of *E. coli*) or 30°C (optimal temperature for chemotaxis, which is dependent on MCPs), as indicated, with vigorous aeration to OD_{600} = 0.7–0.9. Subsequent steps were performed on ice or at 4°C. Minicells and rod cells were separated by differential centrifugation (Dvorak *et al*., 1970) with modifications. Cells were harvested by centrifugation at 1000 *g* for 7 min in a Sorvall SLA-1500 rotor. The resulting pellet (P1) contained undivided filamentous cells and rod cells, whereas the supernatant (S1) was enriched in minicells. The P1 pellet was resuspended in 50 mM Tris-Cl (pH 7.5) buffer (150 ml for 1 l of culture) and centrifuged as above to purify the rod cells further. The S1 supernatant was centrifuged at 14 000 *g* for 15 min to pellet the minicells. The cell pellet was resuspended in 0.15 M NaCl (150 ml for 1 l of culture) and centrifuged at 1000 *g* for 7 min. To increase the purity of minicells, this step was repeated twice or until no pellet was detected. The minicells were pelleted by centrifugation at 14 000 *g* for 15 min, washed in 50 mM Tris-Cl, pH 7.5 (20 ml for 1 l of culture) and pelleted again. The purity of the isolated minicells and rod cells was examined by light microscopy, and the pellets were stored at –80°C.

Preparation of membrane fractions

Cells from 6 l of cell culture were used for each independent cell fractionation experiment. Samples were processed on ice or at 4°C as described previously (Molloy *et al*., 2000; Phadke *et al*., 2001) with minor modifications. Purified rod cells and minicells were resuspended in 90 ml and 10 ml, respectively, of 50 mM Tris-Cl, pH 7.5, containing 1 mM phenylmethylsulphonyl fluoride (PMSF). Cells were disrupted by two passes through a chilled French pressure cell (Aminco) at 16 000 p.s.i. and sonicated at 5 W for 15 s after each

passage through the French pressure cell. The lysate was centrifuged twice at 7000 *g* for 10 min to remove unbroken cells. In general, about 10 and 200 mg of total protein was obtained from minicells and rod cells, respectively, as estimated by a Bradford assay (Bio-Rad). The proteins (10 or 20 mg for minicell and rod cells respectively) were diluted with freshly prepared 0.1 M sodium carbonate (pH 11 without adjustment) to a final volume of 40 ml and stirred slowly on ice for 1 h. Membrane vesicles were collected by ultracentrifugation at 170 000 *g* for 1 h in a Beckman Ti50.2 rotor. The membrane pellet was washed twice by sonication in 1 ml of 50 mM Tris-Cl, pH 7.5, containing 1 mM PMSF and ultracentrifugation (170 000 *g* for 1 h in a Sorvall RP80-AT rotor). The final membrane protein accounted for ≈1/20th–1/25th of the total proteins from rod cells and 1/10th–1/12th of the total proteins from minicells. The membrane pellet was either solubilized immediately for electrophoresis or resuspended in 50 mM Tris-Cl (pH 7.5) containing 10% glycerol and stored at –80°C until use.

Two dimensional electrophoresis

This method was performed as described previously (Molloy *et al*., 2000; Phadke *et al*., 2001) with minor adjustments. Membrane vesicles were solubilized by sonicating in rehydration buffer [7 M urea, 2 M thiourea, 2 mM trybutyl phosphine (TBP; Bio-Rad), 0.5% (v/v) Biolyte 3-10 (Bio-Rad), 40 mM Tris base, 2% (w/v) C8ϕ (4-octyl denzoylamidoproyldimethylammonio-propoane-sulphate), 1% (w/v) Triton X-100]. Membrane samples were incubated at 30°C with shaking for 30 min to 1 h, and the insoluble materials were removed by centrifugation at 17 000 *g* at room temperature for 5 min an SLA-1500 rotor. Rehydration buffer (450 μl) containing 50 μg for analytic gel or 1 mg for preparative gel was rehydrated overnight in each 18 cm immobilized pH gradient strip (IPG; Amersham Pharmacia). Isoelectric focusing (IEF) was carried out for 80 000–100 000 V h^{-1} at a maximum of 6000 V using the Multiphore II system (Amersham Pharmacia) or at maximum of 10 000 V using a Protean IEF cell (Bio-Rad) according to the manufacturer's directions. After IEF, the IPGs were either separated immediately for second dimension or kept at –80°C until use. The IPGs were incubated for 15 min with shaking at room temperature in equilibration buffer [6 M urea, 2% (w/v) SDS, 20% (v/v) glycerol, 0.15 M Bis-tris/0.1 M HCl] containing 1% (w/v) 1,4 dithio-DL-threitol (DTT) followed by 15 min in equilibration buffer containing 3% (w/v) iodoacetamide (IAA). The equilibrated IPGs were separated on 11% SDS–PAGE using Protean II XL multicells. Electrophoresis was carried out at 50 V for 2 h, followed by 110 V for 14–16 h at 4°C. When necessary, the prestained protein markers were loaded at the basic side of the gel. Proteins were visualized by Coomassie brilliant blue G-250 (Molloy *et al*., 2000) for preparative gels or by silver staining (http://www.protana.com/PDF/ASMS/ExAbSilverstain.pdf) for analytical gels.

SDS–PAGE and immunoblot analysis

Glycine–SDS–PAGE was performed as described previously (Sambrook *et al*., 1989). Equal amounts of isolated membrane proteins were resolved on SDS–PAGE and visualized by staining or transferred to nitrocellulose membrane (NEN Life Science) using a semi-dry transfer apparatus (Bio-Rad). Immunoblot analysis was performed according to the manufacturer's manuals and detected by chemiluminescence (NEN Life Science). Dilutions (1:5000) of polyclonal anti-Tar (a gift from D. Koshland) and polyclonal anti-TolC (a gift from Phang C. Tai) antisera were used to detect MCPs and TolC respectively. Monoclonal anti-OmpA and anti-Pal antisera (kindly provided by Judith Hellman) used to detect OmpA and Pal, respectively, were both used at a 1:1000 dilution.

Two-dimensional image comparisons

Gel images were digitized and stored as TIF files with a resolution of 300 d.p.i. using a UMAX Power Look II scanner with MAGIC SCAN software (UMAX) and further manipulated by Adobe PHOTOSHOP. The two-dimensional protein spots were analysed using Z3 2D image analysis system, version 2.0 (Compugen). Protein spots were detected automatically and edited manually to delete artificial spots. The control gel (from rod cell membranes) and experimental gel (from minicell membranes) obtained from the same experimental set were compared by overlaying the images. Using automatic registration followed by manual adjustments, registered images were matched, and a differential enrichment (DE) value of each compared spot was determined. Maximum fit calibration method was used to correct the overall image differences caused by variations in experimental conditions such as protein loading, staining and scanning.

Trypsin in-gel digestion and peptide mass fingerprinting

Protein spots were excised from Coomassie blue or silver-stained gels for analysis. The methods for trypsin in-gel digestion, matrix-assisted laser desorption ionization time-of-flight (MALDI-TOF) mass spectrometry and peptide mass fingerprinting were preformed as described previously (Phadke *et al*., 2001). Briefly, gel pieces containing the protein spots were washed twice in 100 μl of 50% (v/v) acetonitrile (ACN)–100 mM ammonium bicarbonate and digested using 250–500 ng of modified porcine trypsin (Promega) at 37°C overnight. The digested peptides were extracted by incubating in 20 μl of 60% (v/v) ACN–1% (v/v) trifluoroacetic acid (TFA) for 10 min in a sonicator waterbath, concentrated to dryness and resuspended in 6 μl of 3% (v/v) TFA. Each sample (0.8 μl) was co-crystallized with an equal volume of matrix solution [10 mg ml^{-1} (w/v) α-cyano-4-hydroxycannamic acid solution in 50% (v/v) ACN–1% (v/v) TFA] onto a gold-plated MALDI plate (PerSeptive Biosystems). The mass spectrum was analysed on a Voyager-DE STR instrument (PerSeptive Biosystems) run in delayed extraction reflector mode with the following parameters: 1982 laser intensity, 25 kV accelerating voltage, 100 ns delay and a low mass gate of 500 Da. The obtained spectrum was calibrated with proteolytic trypsin monoisotope peaks 842.5 kDa and 2211.1 using DATA EXPLORER (PE Biosystems). The monoisotopic peptide masses were picked up manually or obtained by automation using an in-house virtual instrument created

in the LABVIEW graphical programming language (G. Rymar and P. Andrews, unpublished). The obtained monoisotopic peptide masses were searched against the most recent SWISSPROT or NCBI nr *E. coli* database using the MS-FIT program (http://prospector.ucsf.edu). A maximum of one missed enzymatic cleavage, modification of cysteine residues by carbamidomethylation and possible modification by acrylamide were examined during the searches. A mass accuracy of 150 p.p.m. was used as cut-off unless specified. To be confident about the identity of a protein, a minimum of three matching tryptic peptides was required.

Construction of E. coli *strains encoding OmpW-3HA and YiaF-FLAG*

The *E. coli* K-12 *ompW* (*yciD*) gene, containing its own promoter and open reading frame (ORF) without the stop codon, was amplified by polymerase chain reaction (PCR) using primers OmpW-B1N (5′-CGGGATCCGCAGGTGTTAATT AGCGG-3′) and OmpW-B1C (5′-CGGGATCCCGAAAAC GATATCCTGCTGAG-3′). The PCR product was digested with *Bam*HI and cloned into pBluescript SK+ (Stratagene), digested with the same enzyme. The resulting clone named pJM1860 was verified by sequencing. The *ompW* gene from pJM1860 was amplified using the same forward primer OmpW-B1N and a reverse primer OmpW-HA (5′-GGAATT CCTTAAGCGTAGTCTGGGACGTATGGGTATCTAGAAAAA CGATATCCTGCTGAG) containing the HA epitope tag and cloned into pCR2.1-TOPO TA cloning vector (Invitrogen Life Technologies). From this clone, the *ompW* gene tagged with HA at its C-terminus was excised as an *Eco*RI fragment and subcloned into a low-copy-number vector pGD103 cut with the same enzyme. For the construction of the strain expressing YiaF-FLAG, the *E. coli* K-12 *yiaF* gene, containing its own promoter and ORF without the stop codon, was amplified by PCR using primers YiaF-B1N (5′-CGGGATCCCTTCTGC GAAGGCGTAAATC-3′) and YiaF-B1C (5′-CGGGATCCTT GGGTTGCAGTAACTGCTG-3′). The PCR product was cloned into pCR2.1-TOPO TA cloning vector and verified by sequencing. The *yiaF* gene was excised by *Bam*HI and subcloned into pJM21 a medium-copy, FLAG epitope-tagging plasmid vector cut with the same enzyme.

Microscopy

Cells were processed for immunofluorescence microscopy as described earlier (Maddock and Shapiro, 1993). The dilutions of antisera used were as follows: 1:100 for polyclonal anti-HA antiserum (Zymed), 1:200 for monoclonal anti-Flag antiserum (Sigma-Aldrich), 1:100 for fluorescein-labelled goat anti-mouse antiserum (Jackson ImmunoResearch) and 1:100 for fluorescein-labelled goat anti-rabbit antiserum (Zymed). Cells were visualized by a Nikon E800 microscope using a 100× CFI Plan Apo objective and standard fluorescein isothiocyanate (FITC) and DAPI excitation/emission filter sets. Images were collected using a Hamamatsu ORCA 2 digital camera and Improvision OPENLAB 2 software. Digitized images were imported into Adobe PHOTOSHOP. The purity of rod cell and minicell preparation was assessed by light microscopy using the same microscope and camera mentioned above. Images were captured using the differential interference contrast (DIC) mode.

Acknowledgements

We thank Phil Andrews and Mark Molloy for technical support and stimulating discussion. We are also grateful for the generous gifts of antibodies from D. Koshland, P. C. Tai and J. Hellman, and to Jesse Hay for the use of the immunofluorescence microscope. We are particularly appreciative of the contributions of Antonia Henry during her undergraduate research. This work was supported by grant RSG-01-090-01-MCB from the American Cancer Society.

References

Adler, H.I., Fisher, W.D., Cohen, A., and Hardigree, A.A. (1967) Miniature *Escherichia coli* cells deficient in DNA. *Proc Natl Acad Sci USA* **60:** 321–326.

Alley, M.R., Maddock, J.R., and Shapiro, L. (1992) Polar localization of a bacterial chemoreceptor. *Genes Dev* **6:** 825–836.

Altendorf, K., Stalz, W., Greie, J., and Deckers-Hebestreit, G. (2000) Structure and function of the F(o) complex of the ATP synthase from *Escherichia coli*. *J Exp Biol* **203 Part 1:** 19–28.

Bahloul, A., Meury, J., Kern, R., Garwood, J., Guha, S., and Kohiyama, M. (1996) Co-ordination between membrane oriC sequestration factors and a chromosome partitioning protein, TolC (MukA). *Mol Microbiol* **22:** 275–282.

Bernadac, A., Gavioli, M., Lazzaroni, J.C., Raina, S., and Lloubes, R. (1998) *Escherichia coli tol-pal* mutants form outer membrane vesicles. *J Bacteriol* **180:** 4872–4878.

Bi, E.F., and Lutkenhaus, J. (1991) FtsZ ring structure associated with division in *Escherichia coli*. *Nature* **14:** 161–164.

Bi, E., and Lutkenhaus, J. (1993) Cell division inhibitors SulA and MinCD prevent formation of the FtsZ ring. *J Bacteriol* **175:** 1118–1125.

Bi, E., Dai, K., Subbarao, S., Beall, B., and Lutkenhaus, J. (1991) FtsZ and cell division. *Res Microbiol* **142:** 249–252.

Bouvier, J., Pugsley, A.P., and Stragier, P. (1991) A gene for a new lipoprotein in the *dapA-purC* interval of the *Escherichia coli* chromosome. *J Bacteriol* **173:** 5523–5531.

Bremer, E., Middendorf, A., Martinussen, J., and Valentin-Hansen, P. (1990) Analysis of the *tsx* gene, which encodes a nucleoside-specific channel-forming protein (Tsx) in the outer membrane of *Escherichia coli*. *Gene* **96:** 59–65.

Cantwell, B.J., Draheim, R.R., Weart, R.B., Nguyen, C., Stewart, R.C., and Manson, M.D. (2003) CheZ phosphatase localizes to chemoreceptor patches via CheA-short. *J Bacteriol* **185:** 2354–2361.

Cascales, E., Bernadac, A., Gavioli, M., Lazzaroni, J.C., and Lloubes, R. (2002) Pal lipoprotein of *Escherichia coli* plays a major role in outer membrane integrity. *J Bacteriol* **184:** 754–759.

Cornelis, G.R. (2002) The *Yersinia* Ysc-Yop virulence apparatus. *Int J Med Microbiol* **291:** 455–462.

Delgado, M.A., Solbiati, J.O., Chiuchiolo, M.J., Farias, R.N., and Salomon, R.A. (1999) *Escherichia coli* outer mem-

brane protein TolC is involved in production of the peptide antibiotic microcin J25. *J Bacteriol* **181:** 1968–1970.
Draper, G.C., and Gober, J.W. (2002) Bacterial chromosome segregation. *Annu Rev Microbiol* **56:** 567–597.
Dvorak, H.F., Wetzel, B.K., and Heppel, L.A. (1970) Biochemical and cytochemical evidence for the polar concentration of periplasmic enzymes in a 'minicell' strain of *Escherichia coli*. *J Bacteriol* **104:** 543–548.
Errington, J., Daniel, R.A., and Scheffers, D.J. (2003) Cytokinesis in bacteria. *Microbiol Mol Biol Rev* **67:** 52–65.
Fath, M.J., Zhang, L.H., Rush, J., and Kolter, R. (1994) Purification and characterization of colicin V from *Escherichia coli* culture supernatants. *Biochemistry* **33:** 6911–6917.
Fountoulakis, M., and Gasser, R. (2003) Proteomic analysis of the cell envelope fraction of *Escherichia coli*. *Amino Acids* **24:** 19–41.
Gestwicki, J.E., Lamanna, A.C., Harshey, R.M., McCarter, L.L., Kiessling, L.L., and Adler, J. (2000) Evolutionary conservation of methyl-accepting chemotaxis protein location in bacteria and Archaea. *J Bacteriol* **182:** 6499–6502.
Goodell, E.W., and Schwarz, U. (1977) Enzymes synthesizing and hydrolyzing murein in *Escherichia coli*. Topographical distribution over the cell envelope. *Eur J Biochem* **81:** 205–210.
Green, E.W., and Schaechter, M. (1972) The mode of segregation of the bacterial cell membrane. *Proc Natl Acad Sci USA* **69:** 2312–2316.
Gudmundsdottir, A., Bradbeer, C., and Kadner, R.J. (1988) Altered binding and transport of vitamin B12 resulting from insertion mutations in the *Escherichia coli btuB* gene. *J Biol Chem* **263:** 14224–14230.
Harrison, D.M., Skidmore, J., Armitage, J.P., and Maddock, J.R. (1999) Localization and environmental regulation of MCP-like proteins in *Rhodobacter sphaeroides*. *Mol Microbiol* **31:** 885–892.
Hiraga, S., Niki, H., Ogura, T., Ichinose, C., Mori, H., Ezaki, B., and Jaffe, A. (1989) Chromosome partitioning in *Escherichia coli*: novel mutants producing anucleate cells. *J Bacteriol* **171:** 1496–1505.
Hiraga, S., Niki, H., Imamura, R., Ogura, T., Yamanaka, K., Feng, J., *et al.* (1991) Mutants defective in chromosome partitioning in *E. coli*. *Res Microbiol* **142:** 189–194.
Hu, Z., and Lutkenhaus, J. (1999) Topological regulation of cell division in *Escherichia coli* involves rapid pole to pole oscillation of the division inhibitor MinC under the control of MinD and MinE. *Mol Microbiol* **34:** 82–90.
Kirby, J.R., Niewold, T.B., Maloy, S., and Ordal, G.W. (2000) CheB is required for behavioural responses to negative stimuli during chemotaxis in *Bacillus subtilis*. *Mol Microbiol* **35:** 44–57.
Koppelman, C.M., Den Blaauwen, T., Duursma, M.C., Heeren, R.M., and Nanninga, N. (2001) *Escherichia coli* minicell membranes are enriched in cardiolipin. *J Bacteriol* **183:** 6144–6147.
Kubori, T., Matsushima, Y., Nakamura, D., Uralil, J., Lara-Tejero, M., Sukhan, A., *et al.* (1998) Supramolecular structure of the *Salmonella typhimurium* type III protein secretion system. *Science* **280:** 602–605.
Lawley, T.D., Gordon, G.S., Wright, A., and Taylor, D.E. (2002) Bacterial conjugative transfer: visualization of successful mating pairs and plasmid establishment in live *Escherichia coli*. *Mol Microbiol* **44:** 947–956.
Link, A.J., Robison, K., and Church, G.M. (1997) Comparing the predicted and observed properties of proteins encoded in the genome of *Escherichia coli* K-12. *Electrophoresis* **18:** 1259–1313.
Maddock, J.R., and Shapiro, L. (1993) Polar location of the chemoreceptor complex in the *Escherichia coli* cell. *Science* **259:** 1717–1723.
Meagher, R.B., Tait, R.C., Betlach, M., and Boyer, H.W. (1977) Protein expression in *E. coli* minicells by recombinant plasmids. *Cell* **10:** 521–536.
Mileykovskaya, E., and Dowhan, W. (2000) Visualization of phospholipid domains in *Escherichia coli* by using the cardiolipin-specific fluorescent dye 10-N-nonyl acridine orange. *J Bacteriol* **182:** 1172–1175.
Miller, J.H. (1972) *Experiments in Molecular Genetics*. Cold Spring Harbor, NY: Cold Spring Harbor Laboratory Press.
Molloy, M.P. (2000) Two-dimensional electrophoresis of membrane proteins using immobilized pH gradients. *Anal Biochem* **280:** 1–10.
Molloy, M.P., Herbert, B.R., Slade, M.B., Rabilloud, T., Nouwens, A.S., Williams, K.L., and Gooley, A.A. (2000) Proteomic analysis of the *Escherichia coli* outer membrane. *Eur J Biochem* **267:** 2871–2881.
Molloy, M.P., Phadke, N.D., Chen, H., Tyldesley, R., Garfin, D.E., Maddock, J.R., and Andrews, P.C. (2002) Profiling the alkaline membrane proteome of *Caulobacter crescentus* with two-dimensional electrophoresis and mass spectrometry. *Proteomics* **2:** 899–910.
Pappin, D.J.C., Hojrup, P., and Bleasby, A.J. (1993) Rapid identification of proteins by peptide-mass fingerprinting. *Curr Biol* **3:** 327–332.
Phadke, N.D., Molloy, M.P., Steinhoff, S.A., Ulintz, P.J., Andrews, P.C., and Maddock, J.R. (2001) Analysis of the outer membrane proteome of *Caulobacter crescentus* by two-dimensional electrophoresis and mass spectrometry. *Proteomics* **1:** 705–720.
Pilsl, H., Smajs, D., and Braun, V. (1999) Characterization of colicin S4 and its receptor, OmpW, a minor protein of the *Escherichia coli* outer membrane. *J Bacteriol* **181:** 3578–3581.
Raskin, D.M., and de Boer, P.A. (1997) The MinE ring: an FtsZ-independent cell structure required for selection of the correct division site in *E. coli*. *Cell* **91:** 685–694.
Riede, I., Eschbach, M.L., and Henning, U. (1984) DNA sequence heterogeneity in the genes of T-even type *Escherichia coli* phages encoding the receptor recognizing protein of the long tail fibers. *Mol Gen Genet* **195:** 144–152.
Rosqvist, R., Magnusson, K.E., and Wolf-Watz, H. (1994) Target cell contact triggers expression and polarized transfer of *Yersinia* YopE cytotoxin into mammalian cells. *EMBO J* **13:** 964–972.
Rudner, D.Z., Pan, Q., and Losick, R.M. (2002) A sporulation membrane protein tethers the pro-sigmaK processing enzyme to its inhibitor and dictates its subcellular localization. *Proc Natl Acad Sci USA* **99:** 8701–8706.
Sambrook, J., Fritsch, E.F., and Maniatis, T. (1989) *Molecular Cloning: a Laboratory Manual*, 2nd edn. Cold Spring Harbor, NY: Cold Spring Harbor Laboratory Press.
Shapiro, L., McAdams, H.H., and Losick, R. (2002) Generat-

ing and exploiting polarity in bacteria. *Science* **298:** 1942–1946.

Shiomi, D., Zhulin, I.B., Homma, M., and Kawagishi, I. (2002) Dual recognition of the bacterial chemoreceptor by chemotaxis-specific domains of the CheR methyltransferase. *J Biol Chem* **277:** 42325–42333.

Sourjik, V., and Berg, H.C. (2000) Localization of components of the chemotaxis machinery of *Escherichia coli* using fluorescent protein fusions. *Mol Microbiol* **37:** 740–751.

Steinhauer, J., Agha, R., Pham, T., Varga, A.W., and Goldberg, M.B. (1999) The unipolar *Shigella* surface protein IcsA is targeted directly to the bacterial old pole: IcsP cleavage of IcsA occurs over the entire bacterial surface. *Mol Microbiol* **32:** 367–377.

Urbanus, M.L., Froderberg, L., Drew, D., Bjork, P., de Gier, J.W., Brunner, J., *et al.* (2002) Targeting, insertion, and localization of *Escherichia coli* YidC. *J Biol Chem* **12:** 277 (15): 12718–12723.

Wilson, G., and Fox, C.F. (1971) Membrane assembly in *Escherichia coli*. II. Segregation of preformed and newly formed membrane proteins into cells and minicells. *Biochem Biophys Res Commun* **44:** 503–509.

Yi, L., Jiang, F., Chen, M., Cain, B., Bolhuis, A., and Dalbey, R.E. (2003) YidC is strictly required for membrane insertion of subunits a and c of the F(1)F(0) ATP synthase and SecE of the SecYEG translocase. *Biochemistry* **42:** 10537–10544.

Zhang, L.H., Fath, M.J., Mahanty, H.K., Tai, P.C., and Kolter, R. (1995) Genetic analysis of the colicin V secretion pathway. *Genetics* **141:** 25–32.